

STRUCTURE NOTE

Crystal structure solution of a ParB-like nuclease at atomic resolution

Neil Shaw,¹ Wolfram Tempel,² Jessie Chang,² Hua Yang,² Chongyun Cheng,¹ Joseph Ng,³ John Rose,² Zihe Rao,¹ Bi-Cheng Wang,² and Zhi-Jie Liu^{1*}

¹ National Laboratory of Biomacromolecules, Institute of Biophysics, Chinese Academy of Sciences, Beijing 100101, China

² Southeast Collaboratory for Structural Genomics, Department of Biochemistry and Molecular Biology, University of Georgia, Georgia 30602

³ Laboratory of Structural Biology and Department of Biological Sciences, University of Alabama in Huntsville, Huntsville, Alabama 35899

Key words: *ParB* nuclease; methylation; X-ray structure.

INTRODUCTION

The DNA segregation apparatus of the eukaryotes is well characterized when compared to prokaryotes and archaea, where the components of the machinery and mechanism of segregation is largely unknown. Par (partitioning) B nucleases¹ were initially identified as critical elements of a mechanism involved in the faithful partitioning of plasmid DNA during cell division in the absence of selection pressure.^{1,2} Subsequently, a number of similar proteins have been identified in prokaryotes and archaea carrying out the function of segregation of genomic DNA during cell division. ParB homologs are present in almost all eubacteria. Most of the available information on the segregation of DNA has originated from the studies carried out in *Escherichia coli*,³ *Bacillus subtilis*,⁴ and *Caulobacter crescentus*.⁵ The studies implicate ParA and ParB proteins and their homologs in the DNA segregation process. Mutagenesis studies in *C. crescentus* have indicated ParB to be critical for events preceding cytokinesis. Null mutations of ParB blocked cell division.⁶

At present, no structural information is available on any of the Par proteins known to be involved in the segregation of DNA. To delineate the structural basis for the function of ParB proteins, we cloned a 26 kD ParB-like nuclease from *Pyrococcus furiosus*. The nuclease could be crystallized only after extensive purification followed by

chemical modification. The present work describes the structure of the nuclease solved at atomic resolution. Based on the position of the ligands in the structure, a mechanism for the cleavage of the phosphodiester bond is proposed. The ability of the nuclease to degrade DNA was validated successfully.

MATERIALS AND METHODS

Protein production

A 26 kD ParB-like nuclease was amplified from the genomic DNA of *Pyrococcus furiosus* using PCR and cloned into pET 28a vector (Novagen, USA) as described before.⁷ The gene was expressed with a N-terminal hexa Histidine tag. Protein was purified using Ni-affinity followed by anion exchange chromatography using DEAE Sepharose FF column (Amersham Biosciences, USA). DNA was removed by subjecting the protein to hydroxy-

[†] Atomic co-ordinates and structure factors for the structure reported in the current study have been deposited in the Protein Data Bank under accession code 1VK1.

Grant sponsor: National Institutes of Health; Grant number: 1P50 GM62407; Grant sponsor: National Natural Science Foundation of China; Grant number: 30670427; Grant sponsor: Ministry of Science and Technology of China and the Institute of Biophysics, CAS, China; Grant numbers: 2006AA02A316 (863 Project), 2006CB910901 (973 Project); Grant sponsor: U.S. Department of Energy, Office of Science, Office of Basic Energy Sciences; Grant number: W-31-109-Eng-38; Grant sponsors: University of Georgia Research Foundation, Georgia Research Alliance.

*Correspondence to: Zhi-Jie Liu, National Laboratory of Biomacromolecules, Institute of Biophysics, Chinese Academy of Sciences, Beijing 100101, China. E-mail: zliu@ibp.ac.cn

Received 27 April 2007; Revised 15 May 2007; Accepted 18 May 2007

Published online 29 August 2007 in Wiley InterScience (www.interscience.wiley.com). DOI: 10.1002/prot.21641

apatite chromatography. A final size exclusion chromatography on Sephadex G-75 column (Amersham Biosciences, USA) resulted in a pure, homogenous protein preparation when tested by SDS PAGE and Dynamic Light Scattering (Protein Solutions, USA).

Chemical modification

The nuclease was chemically modified by using a reductive methylation of surface lysines protocol described previously.⁸ Excess chemicals were removed by size exclusion chromatography using a Sephadex G-75 column. After concentration, the methylated protein had a formulation similar to the native protein described previously. A 20 mg/mL methylated protein in 20 mM Tris-HCl, 300 mM NaCl, pH 8.0, was used for crystallization.

Specific activity

The nuclease activity of the ParB protein was determined by dilution method as described previously.⁹ One unit of enzyme activity was defined as the amount of protein required to completely digest 1 µg of pMD-18T plasmid in 60 min at 37°C. The reaction buffer consisted of 50 mM Tris-HCl, pH 8.5, 10 mM CaCl₂, 100 mM NaCl, and 1 mM DTT. Protein concentration was estimated by measuring the absorbance at 280 nm.¹⁰ An extinction coefficient of 28,590 M⁻¹ cm⁻¹ was used to calculate the amount of protein in mg mL⁻¹.

Crystallization

Native (nonmethylated protein) and methylated protein were set up for crystallization in microbatch mode as described¹¹ under identical conditions. A total of 288 commercial sparse matrix screen conditions (Crystal Screen I, Crystal Screen II, MEMFAC, and PEG Ion from Hampton Research, USA; Wizard I and II from DeCode Genetics, USA) were used in the initial screening experiments. All crystallization trials were incubated at 18°C and observed periodically. Diffraction quality crystals were produced from methylated protein using a precipitant solution consisting of 600 mM sodium di-hydrogen phosphate, 2.4M di-potassium hydrogen phosphate, 200 mM sodium chloride, 100 mM HEPES, pH 7.3.

Data collection

The crystals were frozen in liquid nitrogen using a solution containing mother liquor with 25% glycerol as cryo protectant. Derivatives were prepared by addition of a small grain of K₂PtCl₄ to the crystallization drop and subsequent incubation at room temperature for 2 h prior to mounting. Data was collected under cooling at -173°C (Table I) and processed with the HKL2000 suite.¹²

Table I
Data Collection and Refinement Statistics

Dataset	1	2
Derivatization	K ₂ PtCl ₄	Native
X-ray source	RU-H3R	APS 22ID
Detector	R-Axis 4	MAR CCD 225
Crystal-to-detector distance (mm)	122.5	100.0, 130.0
Wavelength (Å)	1.54	1.07
Number of images	360	360, 180
Oscillation width (°)	1.0	0.5, 1.0
Space group	C2	C2
Unit cell parameters		
<i>a</i> (Å)	115.24	115.15
<i>b</i> (Å)	40.08	40.10
<i>c</i> (Å)	66.02	65.67
β (°)	122.32	122.29
Resolution range (highest resolution shell, Å)	11.00–2.30 (2.38–2.30)	50.00–1.20 (1.24–1.20)
Completeness (%)	72.3 (7.0)	80.5 (21.5)
Redundancy	7.1 (2.6)	2.4 (1.1)
<i>R</i> _{sym} (%)	8.5 (17.0)	4.0 (14.0)
<i>I</i> /σ	39.5 (9.8)	34.3 (4.1)
Refinement		
Resolution limits	50.00–1.20	
Number of refined atoms	2015	
<i>R</i> _{work} (<i>R</i> _{free} , %)	16.5 (17.5)	
Bond RMSD lengths (Å)/angles (°)	0.014/1.3	
Mean <i>B</i> value (Å ²)	14.7	
All-atom clash score	1.88	
Ramachandran favored	217/221 (no outliers)	

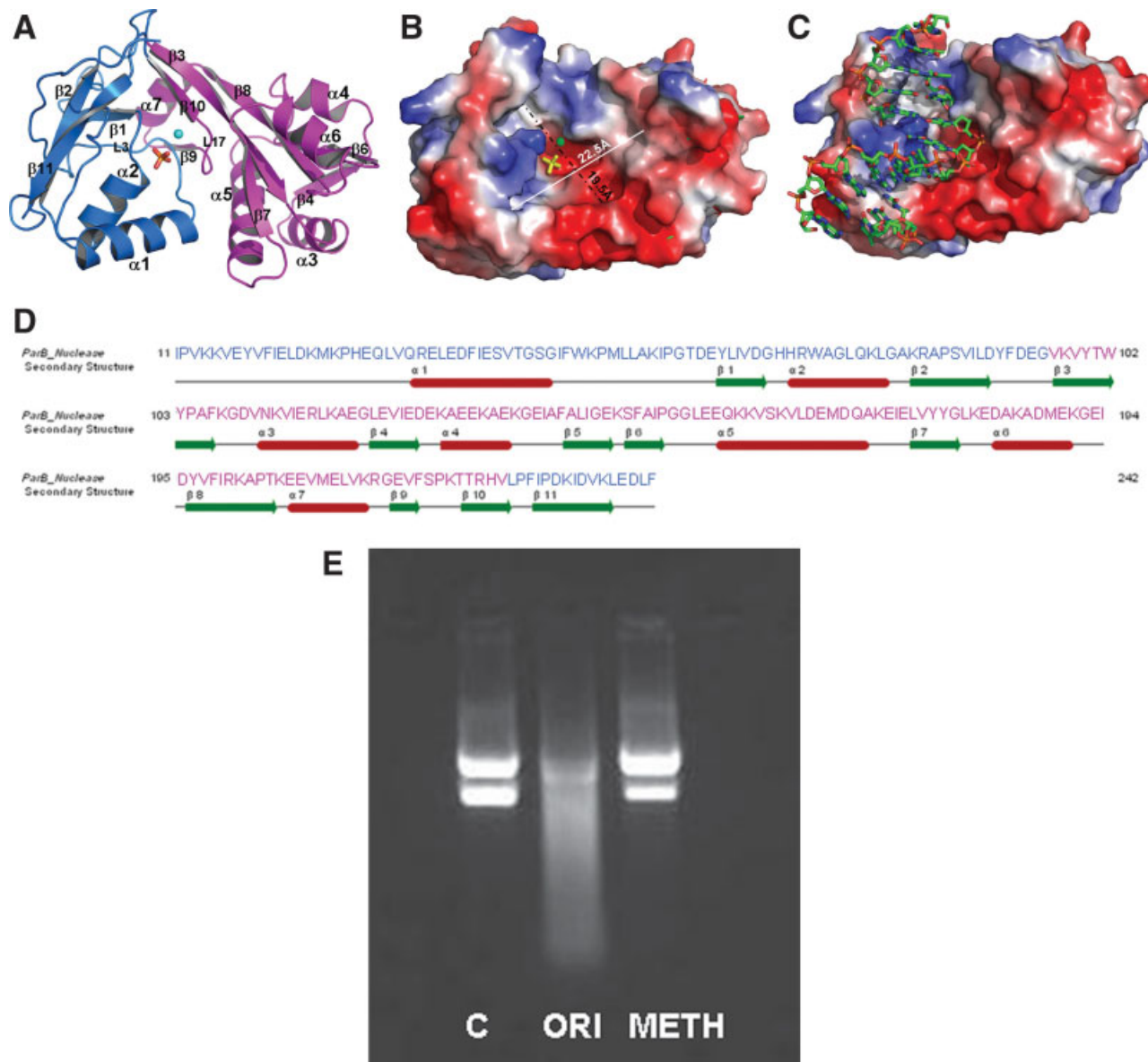
Structure solution and refinement

The initial phases were determined with the Sca2Structure pipeline^{13,14} using the K₂PtCl₄-derivatized crystal (dataset 1) data. Phases were further improved with RESOLVE.¹⁵ The phases were merged with the structure factor amplitudes of the native dataset 2 and an initial model was built with the program ARP/wARP.¹⁶ Rebuilding and refinement were carried out with the programs XFIT¹⁷ and REFMAC,¹⁸ respectively. The structure was validated with MOLPROBITY¹⁹ and PROCHECK²⁰ before deposition with PDB_EXTRACT to the Protein Data Bank.²¹

RESULTS

Structure of the ParB nuclease

The crystal structure of the ParB nuclease was solved by SAD phasing. Three heavy atom sites were identified by SOLVE using the Sca2Structure pipeline. An initial experimental electron density map calculated at 2.0 Å was of extremely high quality as 188 of the 221 residues (85%) could be fitted into the map by ARP/wARP. The structure was refined to 1.2 Å resolution with the final refined model having an *R*-value of 16.5% (*R*-free =

**Figure 1**

Overall structure of ParB nuclease. (A) A cartoon representation of the ParB nuclease structure. The nuclease is made up of seven helices, eleven β -sheets, and numerous loops. The structure could be divided into two domains (colored blue and magenta) according to CATH analysis. (B) A surface electrostatic potential representation of the structure showing the cleft region. The phosphate ligand is buried in a tunnel formed inside the positively charged (blue) cleft. Negative potentials are colored red. The phosphate ligand is shown as sticks and the Ca is represented as a sphere. (C) Putative active site of the ParB-like nuclease with DNA from Eco RV structure (1RVA) superimposed over the cleft region. (D) The primary amino acid sequence of the ParB nuclease annotated with secondary structural elements. Residues making up Domain I are colored blue, while residues forming Domain II are colored magenta. (E) pMD18-T plasmid was treated with purified ParB nuclease (ORI) and the methylated variant (METH) for 60 min at 37°C in a 50 mM Tris-HCl, pH 8.5 buffer, containing 10 mM CaCl_2 , 100 mM NaCl, and 1 mM DTT. A control (C) was set up under identical conditions without the protein. The plasmid was degraded by the ParB nuclease.

17.5%). The Ramachandran plot analysis revealed 217 of the 221 residues were in the most favored region. The data collection and refinement statistics are listed in Table I. Density for the first ten amino acids at the N-terminus was not observed, which is consistent with the PONDR[®] VL-XT analysis of the primary sequence indicating the region to be disordered.

The overall structure consists of seven helices and eleven β -sheets with nineteen loops [Fig. 1(A)]. The structure was classified as mixed $\alpha\beta$ with two-layer sandwich architecture according to CATH.²² Although the topology is similar to other proteins, the structure of the ParB-like nuclease represents a new superfamily. The CATH analysis identified two domains for the protein

with interdigitated secondary structural elements [Fig. 1(A,D)]. Domain I is 101 amino acids long and is made up of two sequence segments. The first segment consists of residues 11 to 96, while the second segment stretches from residues 227 to 242. Domain II is made up of 122 amino acids and includes residues from 97 to 226 [Fig. 1(D)]. Opposite surfaces of the protein are concave in shape, with one surface being more concave than the other. The phosphate ligand is sitting deep inside a tunnel found in a large positively charged cleft region [Fig. 1(B)]. The cleft is 22.5 Å in length and 19.5 Å in width and these dimensions are large enough to accommodate binding of a double-helical DNA moiety. Two loops, L3, and L17 near the edge of the cleft, are juxtaposed to the tunnel and most likely participate in the regulation of access of the molecules to the tunnel [Fig. 1(A)]. The location of the putative active site could be identified by superimposing the structure of Eco RV endonuclease in complex with DNA (PDB code: 1RVA) over the ParB-like nuclease. C α s of 43 residues overlapped with an r.m.s.d. of 2.3 Å. Interestingly, the DNA superimposes over the cleft region of the ParB-like nuclease, suggesting the involvement of the region in binding DNA [Fig. 1(C)]. The minor groove of the DNA is oriented such that the scissile phosphodiester bond is inside the tunnel of the ParB-like nuclease. In the ParB-like nuclease structure, the phosphate ligand is occupying a similar position inside the tunnel. The active site is expected to be located within the tunnel.

DALI analysis²³ for identification of structural neighbors revealed the nuclease to be structurally similar to a chromosome partitioning protein SPO0J (PDB code: 1VZ0) from *Thermus thermophilus*.^{24,25} Although the primary sequence identity was 19%, with a Z score of 3.9, the SPO0J main chain carbons overlapped the C α s of the Domain I of the nuclease with an r.m.s.d. of 2.0 Å (data not shown).

Nuclease activity

ParB nucleases show endo and exo nuclease activities against double- and single-stranded DNA.²⁶ The ability of the protein to degrade DNA was validated by using double-stranded plasmid DNA as substrate [Fig. 1(E)]. The purified nuclease and the chemically modified variant were used for the assay. pMD18-T plasmid was treated with the proteins for 60 min at 37°C. A control was set up under identical conditions without the protein. At the end of the incubation time, the reaction mixture was analyzed by agarose gel electrophoresis. Although the nuclease could degrade the DNA under the assay conditions described in Materials and Methods, the chemical modification of the protein compromised the nucleic acid degradation ability of the protein under identical conditions. The methylated protein could not degrade DNA [Fig. 1(E)]. Even though optimum temper-

ature for the nuclease activity was 37°C, the nuclease retained 60% of its activity at 90°C (data not shown). The ability of the nuclease to cleave DNA at high temperatures was not surprising, since the organism from which the protein was cloned, *Pyrococcus furiosus*, is capable of growing at temperatures as high as 100°C. Thus, the nuclease seems to possess a physiological role in the organism.

The specific activity of the ParB nuclease was 920 U mg⁻¹ under the assay conditions described in Materials and Methods.

DISCUSSION

Although the primary amino acid sequence of the ParB-like nuclease shows very low homology to other nucleases, the overall architecture of the active site shares features essential for the breakage of the DNA backbone with known structures of restriction enzymes.^{27–31} The ligand 302/NA is in an environment and position similar to that of metal ions observed in the 3D structures of a number of restriction enzymes. At the time the coordinates were deposited in the PDB, the ligand was assigned as a Na⁺. The 8-fold co-ordination of the ligand is characteristic of a divalent Ca²⁺ and unlike a divalent Mg²⁺, which shows 6-fold co-ordination. Therefore, the ligand is actually more likely to be a Ca²⁺ rather than Na⁺. Assay of nuclease activity performed using the native protein in the presence of EDTA showed that metal ions were essential for the activity (data not shown). Although Ca²⁺ could be substituted by Mg²⁺ in the assay, the activity was significantly lower in presence of Mg²⁺ (not shown). The phosphate ion was seen bound in a position similar to that of a phosphodiester-bonded phosphate attached to the active site.

During the recovery and purification of the protein, it was observed that the protein bound unusually high amounts of DNA. The initial size exclusion chromatography elution profiles indicated a highly aggregated protein sample bound to nucleic acids. Similar nucleoprotein complexes involved in the partitioning of DNA have been reported for ParB proteins previously.³² The protein could be recovered in a monomeric form after complete removal of the bound DNA using hydroxyapatite chromatography. Only the monomeric form of the protein free of nucleic acids crystallized after the chemical modification. Extensive soaking or cocrystallization experiments with DNA failed to reveal electron density for DNA.

We have determined the crystal structure solution of a ParB-like nuclease at atomic resolution. Functional studies clearly demonstrated the ability of the ParB nuclease to degrade DNA. Although the overall mechanism of segregation of DNA remains unknown, the structure of the ParB-like nuclease protein determined in this study pro-

vides new tools for deciphering the events of DNA segregation at the atomic level. In addition, the nuclease structure determined in this study offers an excellent target for designing new powerful antimicrobial drugs to not only help fight infectious diseases but also contain the spread of drug-resistant plasmids.

ACKNOWLEDGMENTS

Orf pfu392566 encoding the ParB-like nuclease was provided by Michael W. W. Adams' Lab at the Department of Biochemistry and Molecular Biology, University of Georgia. Crystallographic data was collected at Southeast Regional Collaborative Access Team (SER-CAT) 22-ID beamline at the Advanced Photon Source, Argonne National Laboratory. Supporting institutions may be found at www.ser-cat.org/members.html.

REFERENCES

1. Austin S, Ziese M, Sternberg N. A novel role for site-specific recombination in maintenance of bacterial replicons. *Cell* 1981;25:729–736.
2. Gerlitz M, Hrabak O, Schwab H. Partitioning of broad host range Plasmid RP4 is a complex system involving site-specific recombination. *J Bacteriol* 1990;172:6194–6203.
3. Li Y, Sergueev K, Austin S. The segregation of the *Escherichia coli* origin and terminus of replication. *Mol Microbiol* 2002;46:985–996.
4. Webb CD, Teleman A, Gordon S, Straight A, Belmont A, Lin DC, Grossman AD, Wright A, Losick R. Bipolar localization of the replication origin regions of chromosomes in vegetative and sporulating cells of *B. subtilis*. *Cell* 1997;88:667–674.
5. Jensen RB, Shapiro L. The *Caulobacter crescentus smc* gene is required for cell cycle progression and chromosome segregation. *Proc Natl Acad Sci USA* 1999;96:10661–10666.
6. Mohl DA, Easter J, Gober JW. The chromosome partitioning protein, ParB, is required for cytokinesis in *Caulobacter crescentus*. *Mol Microbiol* 2001;42:741–755.
7. Liu ZJ, Tempel W, Ng JD, Lin D, Shah AK, Chen L, Horanyi PS, Habel JE, Kataeva IA, Xu H, Yang H, Chang JC, Huang L, Chang SH, Zhou W, Lee D, Praissman JL, Zhang H, Newton MG, Rose JP, Richardson JS, Richardson DC, Wang BC. The high-throughput protein-to-structure pipeline at SECSG. *Acta Crystallogr D* 2005;61:679–684.
8. Rayment I. Reductive alkylation of lysine residues to alter crystallization properties of proteins. *Methods Enzymol* 1997;276:171–179.
9. Nishioka M, Fujiwara S, Takagi M, Imanaka T. Characterization of two intein homing endonucleases encoded in the DNA polymerase gene of *Pyrococcus kodakaraensis* strain KOD1. *Nucleic Acids Res* 1998;26:4409–4412.
10. Stoscheck CM. Quantitation of protein. *Methods Enzymol* 1990;182:50–69.
11. Chayen NE, Shaw Stewart PD, Maeder DL, Blow DM. An automated system for micro-batch protein crystallization and screening. *J Appl Cryst* 1990;23:297–302.
12. Otwinowski Z, Minor W. Processing of X-ray diffraction data collected in oscillation mode. *Methods Enzymol* 1997;276:307–326.
13. Liu ZJ, Lin D, Tempel W, Praissman JL, Rose JP, Wang BC. Parameter-space screening: a powerful tool for high-throughput crystal structure determination. *Acta Crystallogr D Biol Crystallogr* 2005;61:520–527.
14. Wang BC. Resolution of phase ambiguity in macromolecular crystallography. *Methods Enzymol* 1985;115:90–112.
15. Terwilliger TC. Automated structure solution, density modification and model building. *Acta Crystallogr D* 2002;58:1937–1940.
16. Perrakis A, Morris R, Lamzin VS. Automated protein model building combined with iterative structure refinement. *Nat Struct Biol* 1999;6:458–463.
17. McRee DE. XtalView/Xfit-A versatile program for manipulating atomic coordinates and electron density. *J Struct Biol* 1999;125:156–165.
18. Murshudov GN, Vagin AA, Dodson EJ. Refinement of macromolecular structures by the maximum-likelihood method. *Acta Crystallogr D* 1997;53:240–255.
19. Davis IW, Murray LW, Richardson JS, Richardson DC. MOLPROBITY: structure validation and all-atom contact analysis for nucleic acids and their complexes. *Nucleic Acids Res* 2004;32:W615–W619.
20. Laskowski RA, MacArthur MW, Moss DS, Thornton JM. PROCHECK: a program to check the stereochemical quality of protein structures. *J Appl Crystallogr* 1993;26:283–291.
21. Berman HM, Bhat TN, Bourne PE, Feng Z, Gilliland G, Weissig H, Westbrook J. The Protein Data Bank and the challenge of structural genomics. *Nat Struct Biol Suppl* 2000;7:957–959.
22. Pearl F, Todd A, Sillitoe I, Dibley M, Redfern O, Lewis T, Bennett C, Marsden R, Grant A, Lee D, Akpor A, Maibaum M, Harrison A, Dallman T, Reeves G, Diboun I, Addou S, Lise S, Johnston C, Sillero A, Thornton J, Orengo C. The CATH Domain Structure Database and related resources Gene3D and DHS provide comprehensive domain family information for genome analysis. *Nucleic Acids Res* 2005;33:D247–D251.
23. Holm L, Sander C. Mapping the protein universe. *Science* 1996;273:595–603.
24. Leonard TA, Butler PJ, Lowe J. Structural analysis of the chromosome segregation protein Spo0J from *Thermus thermophilus*. *Mol Microbiol* 2004;53:419–432.
25. Thomas AL, Jonathan B, Löwe J. Bacterial chromosome segregation: structure and DNA binding of the Soj dimer—a conserved biological switch. *EMBO J* 2005;24:270–282.
26. Grohmann E, Stanzer T, Schwab H. The ParB protein encoded by the RP4 par region is a Ca(2+)-dependent nuclease linearizing circular DNA substrates. *Microbiology* 1997;143:3889–3898.
27. Newman M, Strzelecka T, Dorner LF, Schildkraut I, Aggarwal AK. Structure of restriction endonuclease *Bam*HI and its relationship to *Eco*RI. *Nature* 1994;368:660–664.
28. Winkler FK, Banner DW, Oefner C, Tsernoglou D, Brown RS, Heathman SP, Bryan RK, Martin PD, Petratos K, Wilson KS. The crystal structure of *Eco*RV endonuclease and of its complexes with cognate and non-cognate DNA fragments. *EMBO J* 1993;12:1781–1795.
29. Cheng X, Balendiran K, Schildkraut I, Anderson JE. Structure of *Pvu*II endonuclease with cognate DNA. *EMBO J* 1994;13:3927–3935.
30. Wah DA, Hirsch JA, Dorner LF, Schildkraut I, Aggarwal AK. Structure of the multimodular endonuclease *Fok*I bound to DNA. *Nature* 1997;388:97–100.
31. McClarin JA, Frederick CA, Wang BC, Greene P, Boyer HW, Grable J, Rosenberg JM. Structure of the DNA-*Eco*RI endonuclease recognition complex at 3 Å resolution. *Science* 1986;234:1526–1541.
32. Rodionov O, Lobocka M, Yarmolinsky M. Silencing of genes flanking the P1 plasmid centromere. *Science* 1999;283:546–549.